

Bootstrap approximation for the exchange-correlation kernel of time-dependent density functional theory

S. Sharma,* J. K. Dewhurst, A. Sanna, and E. K. U. Gross
Max-Planck-Institut für Mikrostrukturphysik, Weinberg 2, D-06120 Halle, Germany.
 (Dated: October 23, 2018)

A new parameter-free approximation for the exchange-correlation kernel f_{xc} of time-dependent density functional theory is proposed. This kernel is expressed as an algorithm in which the exact Dyson equation for the response as well as a further approximate condition are solved together self-consistently leading to a simple parameter-free kernel. We apply this to the calculation of optical spectra for various small bandgap (Ge, Si, GaAs, AlN, TiO₂, SiC), large bandgap (C, LiF, Ar, Ne) and magnetic (NiO) insulators. The calculated spectra are in very good agreement with experiment for this diverse set of materials, highlighting the universal applicability of the new kernel.

PACS numbers:

The *ab-initio* calculation of optical absorption spectra of nano-structures and solids is a formidable task. The current state-of-the-art is based on many-body perturbation theory. A typical calculation involves two distinct steps: First, the quasi-particle spectral density function is calculated using the *GW* approximation, yielding accurate electron removal and addition energies, and therefore a good prediction for the fundamental gap[1]. In the second step, the Bethe-Salpeter equation (BSE) is solved using the one-body Green's function obtained in the *GW* step. Resonances, corresponding to bound electron-hole pairs called excitons, which have energies inside the gap, can then appear in the spectrum. The two step procedure described above is a well-established method for yielding macroscopic dielectric tensors which are generally in good agreement with experiment[2–7]. Unfortunately, solving the BSE involves diagonalizing a large matrix which couples different Bloch state k -points. As a consequence, the method is computationally expensive.

Time-dependent density functional theory (TDDFT)[8], which extends density functional theory into the time domain, is another method able, in principle, to determine neutral excitations of a system. Although formally exact, the predictions of TDDFT are only as good as the approximation of the exchange-correlation (xc) kernel: $f_{xc}(\mathbf{r}, \mathbf{r}', t - t') \equiv \delta v_{xc}(\mathbf{r}, t) / \delta \rho(\mathbf{r}', t')$, where v_{xc} is the TD exchange-correlation potential and ρ is the TD density. There are several such approximate kernels in existence, the earliest of which is the adiabatic local density approximation (ALDA)[9], where $v_{xc}(\mathbf{r}, t)$ is determined from the usual ground-state local density approximation (LDA), calculated instantaneously for $\rho(\mathbf{r}, t)$. In practice however, the macroscopic dielectric function calculated using this kernel has two well-known deficiencies: the quasi-particle gap is too small and the physics of the bound electron-hole pair is totally missing – in fact ALDA does not improve on the results obtained within the random phase approximation (RPA) which corresponds to the trivial kernel $f_{xc} = 0$ [10]. In the

present work we concentrate on the second of these problems, namely the missing excitonic peak in the spectrum. There have been previous attempts to solve this problem[11], and there exist kernels which correctly reproduce the peaks in the optical spectrum associated with bound excitons. The nano-quanta kernel by Sottile *et al.*[12], derived from the four-point Bethe-Salpeter kernel, is very accurate but has the drawback of being nearly as computationally demanding as solving the BSE itself. The long-range correction (LRC) kernel[13, 14] has a particularly simple form in reciprocal space, $f_{xc} = -\alpha/q^2$, which limits its computational cost. This kernel produces the desired excitonic peak, but depends on the choice of the parameter α , which turns out to be strongly material-dependent, thereby limiting the predictiveness of this approximation. In the present work we propose a new parameter-free approximation for f_{xc} , and demonstrate that this kernel is as accurate as BSE with a computational cost of ALDA.

The exact relationship between the dielectric function ϵ and the kernel f_{xc} for a periodic solid can be written as

$$\begin{aligned} \epsilon^{-1}(\mathbf{q}, \omega) &= 1 + v(\mathbf{q})\chi(\mathbf{q}, \omega) \\ &= 1 + \frac{v(\mathbf{q})\chi_0(\mathbf{q}, \omega)}{1 - [v(\mathbf{q}) + f_{xc}(\mathbf{q}, \omega)]\chi_0(\mathbf{q}, \omega)}, \end{aligned} \quad (1)$$

where v is the bare Coulomb potential, χ is the full response function, and χ_0 is the response function of the non-interacting Kohn-Sham system. All these quantities are matrices in the basis of reciprocal lattice vectors \mathbf{G} . The bootstrap kernel is a frequency-independent approximation given by:

$$f_{xc}^{BS}(\mathbf{q}, \omega) = -\frac{\epsilon^{-1}(\mathbf{q}, \omega = 0)v(\mathbf{q})}{\epsilon_0(\mathbf{q}, \omega = 0) - 1} \quad (2)$$

where $\epsilon_0(\mathbf{q}, \omega) \equiv 1 - v(\mathbf{q})\chi_0(\mathbf{q}, \omega)$. $\epsilon^{-1}(\mathbf{q}, \omega = 0)$ is determined *self-consistently* with Eq. (1). We note that although Eq. (1) is exact, it is useful only when either f_{xc} or ϵ is given; if neither are available then obviously it

cannot be used as a generating equation for both quantities. With the addition of the approximation given by Eq. (2) however, both f_{xc} and ε can be determined from knowledge of χ_0 exclusively. The *modus operandi* for doing so, is to start by setting $f_{xc} = 0$ and then solving Eq. (1) to obtain ε^{-1} . This is then used in Eq. (2) to find a new f_{xc} , and the procedure repeated until self-consistency between the two equations is achieved. The advantages of this form for the kernel is that 1. it has the correct $1/q^2$ behavior[2, 15]; 2. as ε improves from cycle to cycle so does f_{xc} ; 3. the computation cost is minimal, as the most expensive part is the calculation of χ_0 , which needs to be calculated only once; and 4. most importantly, no system-dependent external parameter is required.

The χ_0 in Eqs. (1) and (2) are, in practice, calculated using an approximate ground state xc functional, such as the LDA. To overcome the shortcomings of such an approximation, we further replace the χ_0 by a model response function χ_m coming either from scissors-corrected LDA, or from *GW* or from LDA+*U*. This has the advantage that χ_m , and consequently χ , has the correct gap to begin with. From the formal point of view, this replacement amounts to approximating the TDDFT kernel by

$$f_{xc}^{\text{appr}}(\mathbf{q}, \omega) = \frac{1}{\chi_0(\mathbf{q}, \omega)} - \frac{1}{\chi_m(\mathbf{q}, \omega)} + f_{xc}^{\text{BS}}(\mathbf{q}) \quad (3)$$

Using the method outlined above, optical spectra for various extended systems[16] were calculated using the full-potential linearized augmented plane wave (FP-LAPW) method [17], implemented within the Elk code [18]. Except for the case of solid Ar, a shifted k -point mesh of $15 \times 15 \times 15$ is used to ensure convergence[19]. In the case of solid Ar a shifted mesh of $25 \times 25 \times 25$ k -points was required for convergence of the optical spectrum. All the calculations were performed by scissor shifting the ground-state Kohn-Sham eigenvalues to reproduce the experimental bandgap.

Presented in Fig. 1 are the results for some small (Ge ~ 0.67 eV) to medium (diamond ~ 5.47 eV) bandgap semiconductors. For comparison, experimental data as well as the RPA spectra are also plotted. The experimental data clearly show that all these materials have weakly bound excitons leading to a small shifting of the spectral weight to lower energies compared to RPA. The results from TDDFT with the new kernel exactly follow this trend and are in excellent overall agreement with experiment.

For Ge the TDDFT results are only slightly different from the RPA values which themselves are in agreement with experiment. It is clear that for Ge the RPA is enough and f_{xc} does not significantly improve on the result. This is in complete contrast to the spectrum of Si where the spectral weight is redistributed and, corresponding to experiment, the TDDFT results show an enhanced E_1 peak. The height of the E_2 peak remains marginally overestimated by TDDFT. This overestima-

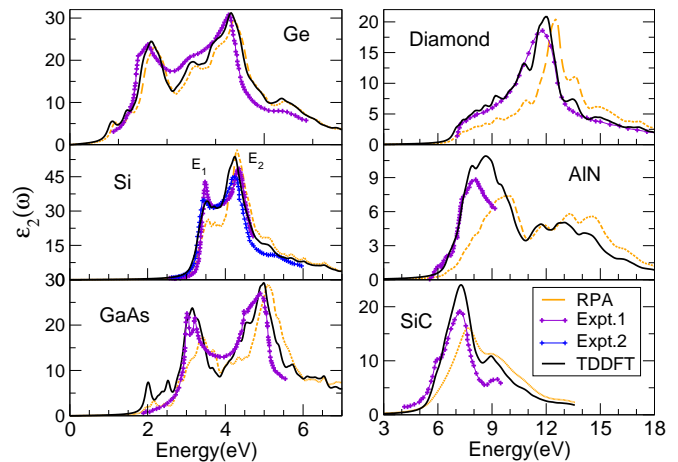


FIG. 1: (Color online) Imaginary part of the dielectric tensor (ε_2) as function[19] of photon energy (in eV). Experimental data are taken from the following sources: Ge from 20, Si from 21 and 22, GaAs from 23, diamond from 24, AlN from 25, and SiC from 26

tion is not particular to the present approximation for f_{xc} , it is also a feature of the BSE-derived kernel [12]. The dielectric function for GaAs is also in very good agreement with experiment – subtle features like the kink at 4.25 eV is well captured by our bootstrap procedure.

The second column of Fig. 1 contains results for medium bandgap insulators. In all these materials a significant redistribution of the spectral weight to lower photon energies is observed. For diamond, the bootstrap procedure correctly leads to an enhancement of the shoulder at low photon energies. The position of the main peak around 12 eV is shifted to lower energies, and the whole spectrum is in near perfect agreement with experiment. AlN is a particularly interesting case, TDDFT shifts the spectral weight to lower energies, and although the height of the peak is too large, the agreement with experiment is considerably better than that obtained by the equivalent BSE calculation [27–29]. For SiC the results show an improvement over the RPA spectrum, but the height of the main peak as well as the shoulder at 9 eV are overestimated. This trend is also observed in previous BSE results[30].

A stringent test for any approximate xc-kernel is in its ability to treat materials with strongly bound excitons. In these cases a new resonant peak appears in the bandgap itself and represents the bound state of an electron-hole pair. Perhaps the most studied test case for this phenomenon is the ionic solid LiF. Other excitonic materials which have also attracted attention and are considered particularly difficult to treat are the noble gas solids. Plotted in the first column of Fig. 2 are the results for three materials of this class: LiF, solid Ar and Ne. What is immediately clear is that the bootstrap procedure, which gave only a slight shift of spectral weight

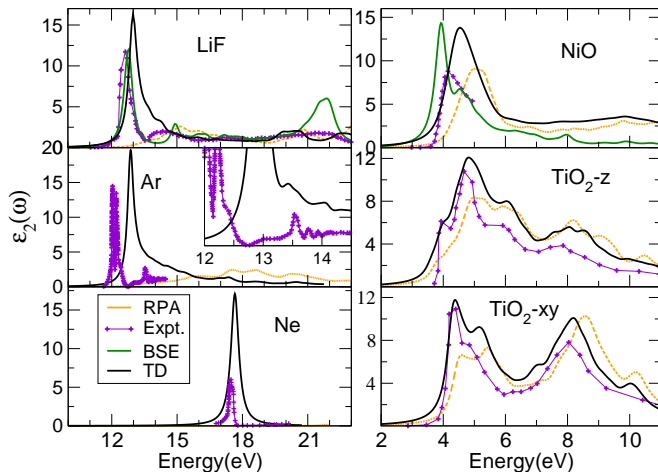


FIG. 2: (Color online) Imaginary part of the dielectric tensor (ϵ_2) as function[19] of photon energy (in eV). Experimental data are taken from the following sources: LiF from 31, Ar and Ne from 32, NiO from 33 and TiO₂ from 34. In the inset a smaller broadening is used to resolve the peaks better[19]

for Ge, now gives rise to an entirely new bound excitonic peak inside the gap in all three cases. The location of the peak, which corresponds to the excitonic binding energy, is also very well reproduced for all these materials.

Despite a good overall agreement we find that for LiF the main peak at 12.5 eV is overestimated, and the peak at 14.3 eV appears as a hump in the TDDFT results. Nevertheless, it is encouraging to note that the BSE spectrum, as well that obtained using the BSE-derived kernel [35], include a spurious peak at around 21 eV which is absent in the present calculations. Noble gas solids have very weak band dispersion and polarizability, which results in very strongly bound electron-hole pairs. In the case of solid Ar, one can observe a strongly localised Frenkel exciton[36] at about 12 eV and a Wannier exciton at about 14 eV. This physics is totally missing within the RPA. Remarkably though, the bootstrap procedure captures both these excitons, although the Wannier exciton is suppressed (see inset). Exactly like in BSE and LRC calculations[36], the Frenkel exciton is under-bound by 0.7eV. Ne has a strongly bound Frenkel exciton and the present calculations capture the corresponding excitonic peak. Similar to the BSE results[37], the height of this peak is overestimated by our TDDFT calculations.

The second column of Fig. 2 consists of some special cases – NiO has an anti-ferromagnetic ground state, and the LDA+ U method is needed to obtain a physically reasonable band structure for this material. This material provides the bootstrap technique with a test of its validity for magnetic materials and also with a check of its performance when the scissors-corrected LDA is replaced by LDA+ U , where U is chosen to reproduce the experimental gap. It is clear from Fig. 2 that the bootstrap method leads once again to the correct excitonic bind-

ing energy. The experimental data for NiO are rather old and substantially broadened [33], and, assuming the veracity of these data, both TDDFT and BSE[38] overestimate the peak height. It is worth noting that the BSE spectrum is redshifted relative to experiment, while the TDDFT spectrum is correctly positioned. Results for the anatase phase of TiO₂ are also presented in Fig. 2. This material is important for its industrial use in photovoltaics and has been well characterized using the BSE and GW method [39, 40] as well as experiment[34]. TiO₂ is a useful test for the bootstrap method due to its non-cubic unit cell, which leads to directional anisotropy in the optical spectrum. As can be seen in Fig. 2, the bootstrap method captures this anisotropy very well indeed. Even subtle features like the small shoulder at ~ 4 eV in the out-of-plane dielectric function, which is missing in the in-plane case, are well reproduced. We find that our peak heights are slightly overestimated, which is also the case for the BSE results [39].

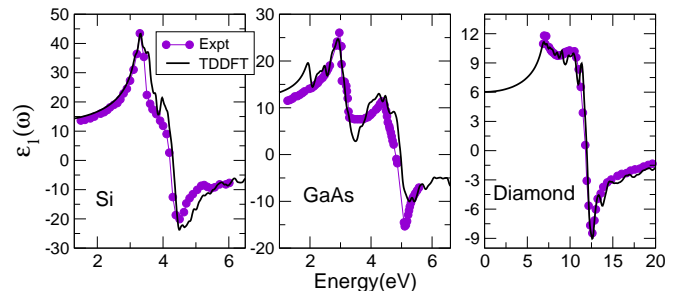


FIG. 3: (Color online) Real part of the dielectric tensor (ϵ_1) as function of photon energy (in eV) for Si, GaAs and diamond.

It is also interesting to compare the real part of the dielectric function with available experimental data. Results for Si, GaAs and diamond are presented in Fig. 3. In all three cases, TDDFT results are in excellent agreement with the experimental data. We note that in the low frequency regime (below 2eV) the TDDFT results for GaAs deviate from experiments in exactly the same manner as found for the LRC kernel[30].

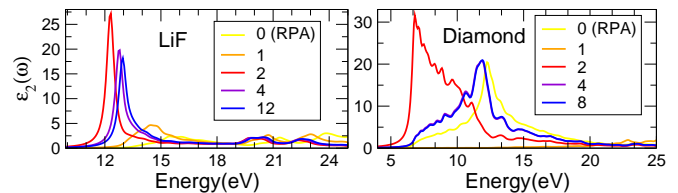


FIG. 4: (Color online) Imaginary part of the dielectric tensor (ϵ_2) as function of photon energy (in eV) for LiF and diamond. ϵ_2 is plotted at various steps of the self-consistency.

The effect of the bootstrap procedure can be seen in Fig. 4 where ϵ_2 is plotted at each step of the self-consistency. As specified, the starting point is $f_{xc} = 0$ which yields the RPA spectrum in the first iteration.

From then on, ε_2 changes substantially until convergence, indicating the importance of the self-consistency.

An interesting point to note about Eq. (2) is that this form of f_{xc} is related to the two existing TDDFT kernels which capture the excitonic physics. In particular it corresponds to the LRC kernel when $\alpha = 4\pi\varepsilon^{-1}/(\varepsilon_0 - 1)$, and ε is determined self-consistently. Also, like for the LRC kernel, the $\mathbf{G} = \mathbf{G}' = 0$ part of f_{xc} is by far the most important contribution. This also explains the fast convergence of the optical spectra with respect to the reciprocal lattice vectors included in f_{xc} . Comparing our kernel to the BSE-derived approximation, in both cases the f_{xc} is proportional to the screened Coulomb matrix elements $\varepsilon^{-1}v$. Choosing f_{xc} to be proportional to the screened Coulomb interaction was also exploited by Turkowski *et al.* (see Eq. 1 and 15 of Ref. 41). There remain several interesting aspects of the bootstrap method to be explored in the future: 1. the finite \mathbf{q} version of this approximation to determine the energy loss spectrum; 2. performance of this approximation for two-dimensional systems, like graphene sheets or even nanotubes where excitonic effects are particularly strong; 3. to study the possibility of making this functional frequency-dependent; and 4. to explore analogous construction of f_{xc} for finite systems and study its performance for excitonic spectra in molecular aggregates.

Thus we have demonstrated that the bootstrap procedure gives a parameter-free TDDFT kernel which yields very accurate optical spectra. The same functional which produces a small shift, relative to the RPA, in the absorption edge of Ge, also generates an entirely new excitonic peak within the bandgap of LiF, Ar and Ne. This indicates that the bootstrap kernel has wide applicability. The same quality of results can also be obtained by solving the BSE, but the present method is highly desirable from the point of view of computation effort.

* Electronic address: sharma@mpi-halle.mpg.de

- [1] L. Hedin, Phys. Rev. **139**, 796 (1965).
- [2] G. Onida, L. Reining, and A. Rubio, Rev. Mod. Phys. **74**, 601 (2002).
- [3] G. Onida, L. Reining, R. W. Godby, R. D. Sole, and W. Andreoni, Phys. Rev. Lett. **75**, 818 (1995).
- [4] S. Albrecht, L. Reining, R. D. Sole, and G. Onida, Phys. Rev. B **80**, 4510 (1998).
- [5] L. X. Benedict, E. L. Shirley, and R. B. Bohn, Phys. Rev. B **57**, R9385 (2000).
- [6] M. Rohlfing and S. G. Louie, Phys. Rev. Lett. **81**, 2312 (1998).
- [7] A. Marini, C. Hogan, m. Grüning, and D. Varsano, Comp. Phys. Comm. **180**, 1392 (2009).
- [8] E. Runge and E. K. U. Gross, Phys. Rev. Lett. **52**, 997 (1984).
- [9] E. K. U. Gross, F. J. Dobson, and M. Petersilka, Density Functional Theory (Springer, New York) (and references therein) (1994).
- [10] V. I. Gavrilenko and F. Bechstedt, Phys. Rev. B **55**, 4343 (1997).
- [11] S. Botti, A. Schindlmayr, R. D. Sole, and L. Reining, Rep. Prog. Phys. **70**, 357 (2007).
- [12] F. Sottile, V. Olevano, and L. Reining, Phys. Rev. Lett. **91**, 056402 (2003).
- [13] L. Reining, V. Olevano, A. Rubio, and G. Onida, Phys. Rev. Lett. **88**, 066404 (2002).
- [14] S. Botti, A. Fourreau, F. Nguyen, Y. Renault, F. Sottile, and L. Reining, Phys. Rev. B **72**, 125203 (2005).
- [15] P. Ghosez, X. Gonze, and R. W. Godby, Phys. Rev. B **56**, 12811 (1997).
- [16] following experimental lattice parameters (in a.u.) were used: Ge 10.69, Si 10.26, GaAs 10.6870, AlN 8.2760, SiC 8.2386, diamond 6.7274, LiF 7.60804, Ar 10.030, Ne 8.440, NiO 7.893389 and TiO2 a=7.1511, c=8.9899.
- [17] D. J. Singh, Planewaves Pseudopotentials and the LAPW Method, Kluwer Academic Publishers, Boston (1994).
- [18] (2004), URL <http://elk.sourceforge.net>.
- [19] The calculated spectra was broadened by (in eV): Ge 0.11, Si 0.05, GaAs 0.1, AlN 0.2, SiC 0.23, diamond 0.22, LiF 0.16, Ar 0.2 (and 0.1 for inset), Ne 0.2, NiO 0.2 and TiO2 0.16.
- [20] D. E. Aspnes and A. A. Studna, Phys. Rev. B **27**, 985 (1983).
- [21] P. Lautenschlager, M. Garriga, L. Vina, and M. Cardona, Phys. Rev. B **36**, 4821 (1987).
- [22] D. E. Aspnes and A. A. Studna, Phys. Rev. B **27**, 985 (1983).
- [23] P. Lautenschlager, M. Garriga, S. Logothetidis, and M. Cardona, Phys. Rev. B **35**, 9174 (1987).
- [24] D. Edwards and H. Philipp, Handbook of Optical Constants of Solids, edited by E.D. Palik (Academic Press, Orlando, 1985).
- [25] V. Cimalla, V. Lebedev, U. Kaiser, R. Goldhahn, C. Förster, J. Pezoldt, and O. Ambacher, Phys. Status Solidi C **2**, 2199 (2005).
- [26] S. Logothetidis and J. Petalas, J. Appl. Phys. **80**, 1768 (1996).
- [27] F. Bechstedt, K. Seino, P. H. Hahn, and W. G. Schmidt, Phys. Rev. B **72**, 245114 (2005).
- [28] P. H. Hahn, K. seino, W. G. Schmidt, J. Furthmüller, and F. Bechstedt, Phys. Stat. Sol. (b) **242**, 2720 (2005).
- [29] R. Laskowski and N. E. Christensen, Phys. Stat. Sol. (b) **244**, 17 (2007).
- [30] S. Botti, F. Sottile, N. Vast, V. Olevano, L. Reining, H. Weissker, A. Rubio, G. Onida, R. D. Sole, and R. W. Godby, Phys. Rev. B **69**, 155112 (2004).
- [31] D. Roessler and W. Walker, J. Opt. Soc. Am. **57**, 835 (1967).
- [32] B. Sonntag, in Rare Gas Solids, edited by M. L. Klein and J. A. Venables (Academic Press, London, 1976), Vol. II, pp. 10211117.
- [33] R. J. Powell and W. E. Spicer, Phys. Rev. B **2**, 2182 (1970).
- [34] N. Hosaka, T. Sekiya, C. Satoko, and S. Kurita, J. Phys. Soc. Jpn. **66**, 877 (1997).
- [35] A. Marini, R. D. Sole, and A. Rubio, Phys. Rev. Lett. **91**, 256402 (2003).
- [36] F. Sottile, M. Marsili, V. Olevano, and L. Reining, Phys. Rev. B **76**, R161103 (2007).
- [37] S. Galamic-Mulaomerovic and C. H. Patterson, Phys. Rev. B **72**, 035127 (2005).

- [38] C. Rödl, Elektronische und exzitonische Anregungen in magnetischen Isolatoren (page 74) (2010).
- [39] H. M. Lawler, J. J. Rehr, F. Vila, S. D. Dalosto, E. L. Shirley, and Z. H. Levin, Phys. Rev. B **78**, 205108 (2008).
- [40] W. Kang and M. S. Hybertsen, Phys. Rev. B **82**, 085203 (2010).
- [41] V. Turkowski, A. Leonardo, and C. A. Ullrich, Phys. Rev. B **79**, 233201 (2009).